

Testing consistency of $\Omega_b h^2$ in the Planck data

Pavel Motloch¹

¹Canadian Institute for Theoretical Astrophysics, University of Toronto, M5S 3H8, ON, Canada

We find that the cosmic microwave background temperature and polarization power spectra measurements from Planck constrain the parameter $\Omega_b h^2$ mostly through: A) the amplitude of Thomson scattering and B) a factor that ensures Thomson scattering does not violate momentum conservation of the baryon-photon fluid. This allows us to obtain two distinct but comparably strong constraints on $\Omega_b h^2$ from the Planck data alone. They are consistent, showing robustness of the Planck $\Omega_b h^2$ constraint. We can alternatively rephrase these constraints as A) the change of the Thomson scattering cross section since recombination is less than $\sim 2\%$ and B) momentum during recombination is conserved to better than $\sim 2\%$ by Thomson scattering. Decoupling the eight various ways in which $\Omega_b h^2$ affects the Planck data leads to slightly higher H_0 than in the standard analysis, (69.1 ± 1.6) km/s/Mpc, but the overall consistency of all $\Omega_b h^2$ constraints does not suggest any problem with the standard cosmological model.

I. INTRODUCTION

Physical density of baryons $\Omega_b h^2$ is one of the parameters of the standard cosmological model (Λ CDM). Currently, it is best constrained by the cosmic microwave background (CMB) temperature and polarization power spectra measured by the Planck satellite [1]:

$$\Omega_b h^2 = 0.02236 \pm 0.00015. \quad (1)$$

Measurements of primordial deuterium abundance from absorption in quasar spectra [2] allows for competitive determinations, either

$$\Omega_b h^2 = 0.02166 \pm 0.00015 \pm 0.00011 \quad (2)$$

or

$$\Omega_b h^2 = 0.02235 \pm 0.00016 \pm 0.00033, \quad (3)$$

depending on whether the value of $d(p, \gamma)^3\text{He}$ reaction rate used to get the constraint is calculated theoretically (2) or measured (3). The first error corresponds to uncertainty in the deuterium abundance measurement and the second to the uncertainty of the nuclear rates and other parts of the big-bang nucleosynthesis (BBN) calculation.

While the difference between the Planck value (1) and the BBN value (2) is almost reaching the 3σ level, this could just signal a problem with the theoretical calculation of the $d(p, \gamma)^3\text{He}$ rate or a statistical fluctuation, especially given the less precise BBN constraint (3).

However, this discrepancy motivated us to look deeper into how exactly do the CMB data constrain $\Omega_b h^2$ or, equivalently, through which physical processes does $\Omega_b h^2$ enter the calculation of the CMB power spectra. Additionally, we are interested in finding relative constraining power of these individual physical processes. Beyond gaining theoretical understanding, unless the baryonic constraints are strongly dominated by a single physical process, we will be able to derive *several* constraints on $\Omega_b h^2$ using the Planck data *alone*. It is not assured a priori that these should all mutually agree. This would allow us to check the internal consistency of the Planck

data, with the hope of shedding additional light into the aforementioned $\Omega_b h^2$ tension between Planck and deuterium measurement (2). Additionally, if a discrepancy is found it may offer a clue on how to resolve the tension between the local measurement of today's value of the Hubble constant, $H_0 = (74.0 \pm 1.4)$ km/s/Mpc [3], and its value inferred from CMB within the standard cosmological model, $H_0 = (67.3 \pm 0.6)$ km/s/Mpc [1]. In case physics beyond the standard model is responsible for this tension, time around recombination has been singled out as the most promising place to investigate [4] and our analysis might be able to pick up signals of such new physics.

This paper is organized as follows: In § II we summarize the data used and outline the general strategy of our analysis. In § III we review the well known steps in the calculation of the CMB power spectra, list all the ways in which $\Omega_b h^2$ enters this calculation and describe how we alter the standard computer codes for our analysis. We present our results in § IV and discuss them in § V.

II. DATA, ANALYSIS AND SEVERAL $\Omega_b h^2$ PARAMETERS

To constrain values of cosmological parameters, we use the legacy likelihoods `plik_rd12_HM_v22b_TTTEEE`, `small1_100x143_offlike5_EE_Aplanck_B` and `commander_dx12_v3_2_29` based on the Planck satellite measurements of the CMB temperature and polarization power spectra [5].

We use CosmoMC [6] to obtain posterior probability distributions for the cosmological parameters, using theoretical predictions calculated with CAMB [7].

We use flat uninformative priors for $\Omega_c h^2$, the physical cold dark matter (CDM) density; n_s , the tilt of the scalar power spectrum; $\ln A_s$, its log amplitude at $k = 0.05 \text{ Mpc}^{-1}$; τ_{rei} , the optical depth through reionization, and θ_{MC} , the effective angular scale of the sound horizon at recombination. We use default priors for the nuisance parameters. We run the Markov chains until the Gelman-Rubin statistic $R - 1$ drops below 0.01.

We consider eight $\Omega_b h^2$ parameters, each affecting CMB power spectra in one of the eight different ways that are listed in § III B. Standard analysis would correspond to forcing all these parameters to have an identical value, we allow them to differ. Each of these parameters is sampled with a flat prior [0.0172, 0.0272] that safely includes the independent BBN constraints (2) and (3).

Because Planck data do not have sufficient power to detect nonzero neutrino masses (e.g. [8]), we neglect neutrino masses for simplicity of the discussion and analysis. Additionally, we only consider flat cosmologies with adiabatic initial conditions and no tensor modes.

III. HOW BARYONS AFFECT CMB

In this section we start by reminding the reader the steps involved in the calculation of the CMB power spectra (e.g. [9]). Then we list all the ways in which $\Omega_b h^2$ enters the calculation and finish by describing our implementation.

In this section we use standard symbols to denote physical quantities, with perturbations in the synchronous gauge: a is the scale factor, $\Omega_{b,c,\gamma,\nu}$ are fractions of today's energy density in baryons, CDM, photons and neutrinos, h and η are the scalar gravitational potentials, $\delta_{b,c}$ are fractional overdensities of baryons and CDM, v_b is velocity of baryons, $\Theta_{\gamma\ell}$ and $\Theta_{\nu\ell}$ are multipole moments of the photon and massless neutrino hierarchies. As usual, we work with Fourier space variables.

In all equations, dot represents a derivative with respect to the conformal time.

A. Steps in the CMB power spectra calculation

As is well known, calculation of the CMB power spectra proceeds in several steps. First, background quantities such as time dependence of the scale factor and free electron fraction are calculated. Because of the small amplitude of perturbations around the homogeneous and isotropic background, it is sufficient to focus on linear perturbations, with distinct Fourier modes decoupled. For each wavenumber \vec{k} it is necessary to solve a set of ordinary differential equations. Because of the assumed isotropy, only the amplitude of the wavenumber k plays a role. Once solutions for a representative set of wavenumbers are known, they are used to calculate sources of the observed temperature and polarization fields [10]. Starting with power spectra of the initial curvature perturbations and integrating over k , one gets the unlensed CMB power spectra. These are then converted into the lensed power spectra following [11].

B. Effects of $\Omega_b h^2$

By going through the details of the CMB power spectra calculation summarized above and checking with the source code of CAMB, we have found the following eight ways in which $\Omega_b h^2$ enters the calculation of the CMB power spectra:

1. Background expansion

Baryons enter the time dependence of the scale factor through the Friedmann equation,

$$\frac{\dot{a}}{a^2} = H_0 \sqrt{\frac{\Omega_b}{a^3} + \frac{\Omega_c}{a^3} + \frac{\Omega_\gamma}{a^4} + \frac{\Omega_\nu}{a^4} + \Omega_\Lambda}, \quad (4)$$

where we assume a flat Universe and thus

$$\Omega_\Lambda = 1 - \Omega_b - \Omega_c - \Omega_\gamma - \Omega_\nu. \quad (5)$$

2. Helium abundance

Helium abundance as calculated in BBN is dependent on the baryon density, $Y_p(\Omega_b h^2, \dots)$, though this dependence is rather weak, as is well known.

3. Recombination

The time dependence of the free electron fraction x_e calculated in recombination codes such as Recfast [12] depends on the amount of baryons in the Universe. Reader can see this easily for example on the simplest model of recombination — Saha equation — in which

$$\frac{x_e^2}{1 - x_e} = \frac{1}{n_b} \left(\frac{m_e T}{2\pi} \right)^{3/2} e^{-\epsilon_0/T}, \quad (6)$$

where m_e is the electron mass, T CMB temperature, ϵ_0 hydrogen ionization energy and $n_b \propto \Omega_b$.

4. Evolution of metric perturbations

Because baryons contribute to the energy density of the Universe, their perturbations contribute to the evolution of the metric potentials, specifically

$$\begin{aligned} \frac{\dot{a}}{a} \dot{h} &= 2k^2 \eta + 3H_0^2 \left(\frac{\Omega_b}{a} \delta_b + \frac{\Omega_c}{a} \delta_c + \frac{\Omega_\gamma}{a^2} \Theta_{\gamma 0} + \frac{\Omega_\nu}{a^2} \Theta_{\nu 0} \right) \\ \dot{\eta} &= \frac{3H_0^2}{2k} \left(\frac{\Omega_b}{a} v_b + \frac{\Omega_\gamma}{a^2} \Theta_{\gamma 1} + \frac{\Omega_\nu}{a^2} \Theta_{\nu 1} \right). \end{aligned} \quad (7)$$

Considering the two equations separately, we count these as two distinct effects.

5. Thomson scattering

Another way in which the amount of baryons in the Universe affects CMB is through the amplitude of the Thomson scattering, as manifested for example in the equation of motion for the first photon multipole,

$$\dot{\Theta}_{\gamma 1} = \frac{k\Theta_{\gamma 0}}{3} - \frac{2k\Theta_{\gamma 2}}{3} + an_e\sigma_T \left(\frac{4}{3}v_b - \Theta_{\gamma 1} \right). \quad (8)$$

Here n_e is the free electron density and σ_T Thomson scattering cross section. The amplitude of the scattering, $an_e\sigma_T$, is proportional to Ω_b .

6. Momentum conservation

Due to different densities of baryons and photons, the interaction term in the baryonic equation of motion

$$\dot{v}_b = -\frac{\dot{a}}{a}v_b + c_s^2 k\delta_b + Ran_e\sigma_T \left(\frac{3}{4}\Theta_{\gamma 1} - v_b \right) \quad (9)$$

is multiplied by $R = \frac{4\Omega_\gamma}{3\Omega_b a}$ to ensure momentum conservation, i.e. that the total momentum of the baryon-photon fluid is not changed by mutual interaction through Thomson scattering. As usual, c_s^2 is baryonic sound speed.

With $an_e\sigma_T$ already discussed, R brings additional dependence on the baryonic density.

7. Non-linear lensing

Finally, the lensing corrections due to non-linear effects [13] also depend on $\Omega_b h^2$, although this dependence is not expected to be significant.

C. Implementation

Having found the eight ways in which $\Omega_b h^2$ enters the calculation of the CMB power spectra, we discuss here changes to the standard computer codes — CosmoMC and CAMB — that allow us to explore how $\Omega_b h^2$ is constrained by the CMB.

In the big picture view, we want to replace a single $\Omega_b h^2$ parameter that is part of the standard calculation by eight parameters $\Omega_b^X h^2$, with each entering the calculation through a different physical process. All these parameters and what they control are listed in Table I.

Most of the changes to the codes are straightforward and only consist of duplicating variables and tracking them through the calculations, but we want to comment on two non-trivial changes: setting the initial conditions and calculating time derivatives of shear.

Initial conditions can be obtained by expanding all variables as polynomials in conformal time and inverse

TABLE I. List of $\Omega_b^X h^2$ parameters

Parameter	Affects CMB power spectra through
$\Omega_b^{\text{EXP}} h^2$	Background expansion (4)
$\Omega_b^{\text{BBN}} h^2$	Helium abundance
$\Omega_b^{\text{REC}} h^2$	Recombination calculation of x_e
$\Omega_b^{\text{ETA}} h^2, \Omega_b^{\text{H}} h^2$	Evolution equations for η, h (7)
$\Omega_b^{\text{THO}} h^2$	Amplitude of Thomson scattering
$\Omega_b^{\text{R}} h^2$	Momentum conservation factor R
$\Omega_b^{\text{HALO}} h^2$	Non-linear lensing

opacity $(an_e\sigma_T)^{-1}$ [14] and matching the leading coefficients in the evolution equations. After generalizing the results of Appendix B of [14] to our setup, we find that the following changes need to be made to the initial conditions at conformal time τ_{ini} as implemented in CAMB:

$$\begin{aligned} \delta_\gamma^{\text{ini}} &= -\frac{2k^2\tau_{\text{ini}}^2}{3} \left[1 + \frac{\omega\tau_{\text{ini}}(\Omega_b^{\text{EXP}} - 3\Omega_b^{\text{H}} - 2\Omega_c)}{10(\Omega_b^{\text{EXP}} + \Omega_c)} \right] \quad (10) \\ \Theta_{\nu 2}^{\text{ini}} &= \frac{4k^2\tau_{\text{ini}}^2}{3(4R_\nu + 15)} \left[1 + \frac{\omega\tau_{\text{ini}}(4R_\nu C_1 - 5C_0)}{8(\Omega_b^{\text{EXP}} + \Omega_c)(2R_\nu + 15)} \right], \quad (11) \end{aligned}$$

where we have introduced

$$R_\nu = \frac{\Omega_\nu}{\Omega_\nu + \Omega_\gamma} \quad (12)$$

$$\omega = \frac{H_0(\Omega_b^{\text{EXP}} + \Omega_c)}{\sqrt{\Omega_\gamma + \Omega_\nu}} \quad (13)$$

$$C_0 = 6\Omega_b^{\text{ETA}} - 7\Omega_b^{\text{EXP}} + 9\Omega_b^{\text{H}} - 6\Omega_b^{\text{R}} + 2\Omega_c \quad (14)$$

$$C_1 = -2\Omega_b^{\text{ETA}} + 5\Omega_b^{\text{EXP}} - 3\Omega_b^{\text{H}} + 2\Omega_b^{\text{R}} + 2\Omega_c. \quad (15)$$

Because of the way CAMB implements initial conditions, all other initial conditions are automatically correct, e.g. they are adiabatic. It is easy to see that when all Ω_b^X are equal, we reproduce the standard result.

The second nontrivial change is calculating time derivatives of shear σ , defined as

$$\sigma = \frac{\dot{h} + 6\dot{\eta}}{2k}. \quad (16)$$

These derivatives are involved in second order tight coupling scheme [14], and when calculating CMB sources and the gravitational lensing potential. In CAMB, the derivatives are calculated from the Einstein equation

$$k\dot{\sigma} + 2\frac{\dot{a}}{a}k\sigma - k^2\eta = -3H_0^2 \left(\frac{\Omega_\nu}{a^2}\Theta_{\nu 2} + \frac{\Omega_\gamma}{a^2}\Theta_{\gamma 2} \right), \quad (17)$$

that is exact in general relativity. Although the c_s^2 terms in the evolution equations as implemented in CAMB break (17) and CAMB is thus slightly inconsistent, this does not affect constraints on cosmological parameters when using Planck data [15]. For this reason, we ignore this issue in this work. Our altered equations of motion

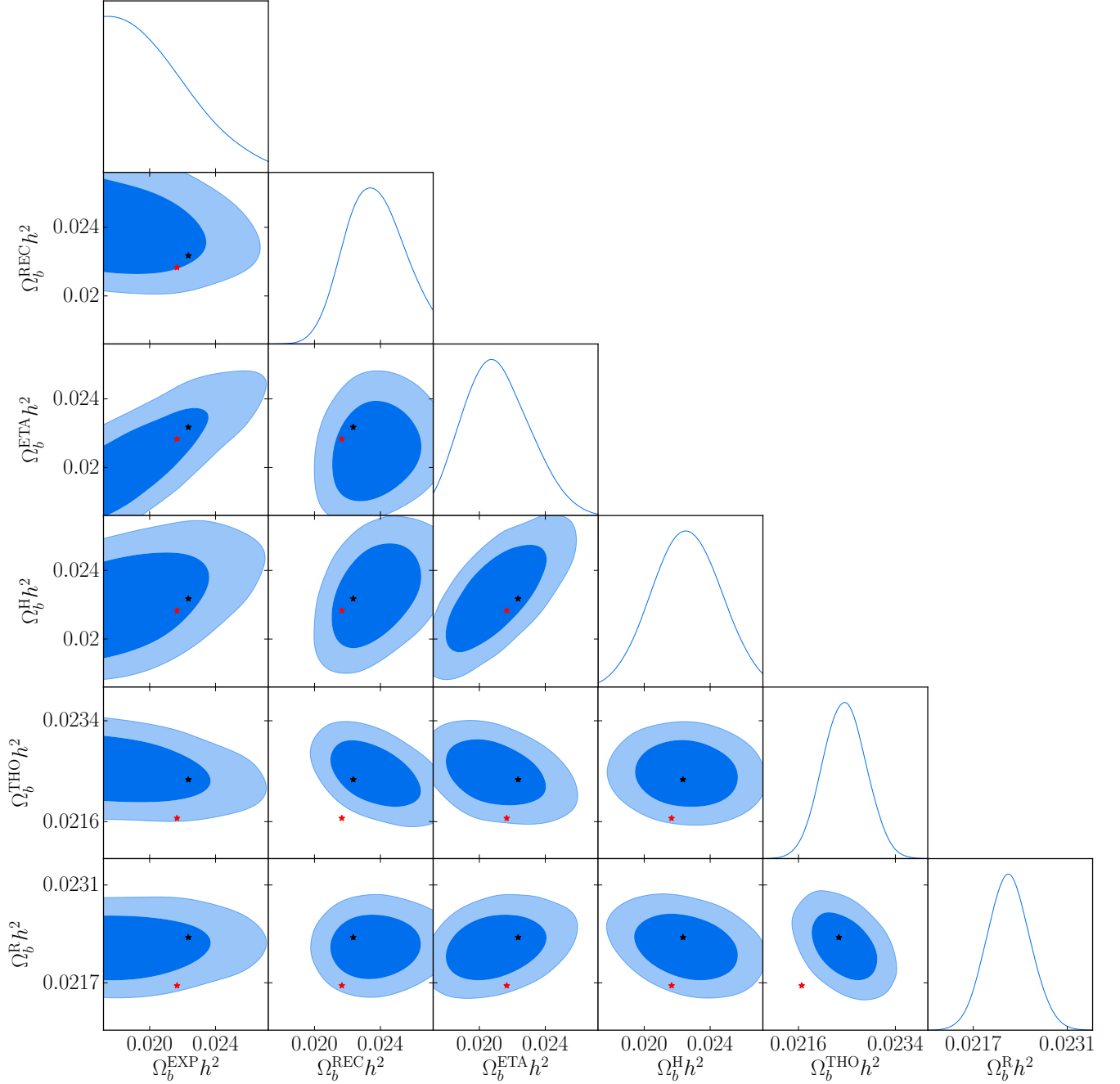


FIG. 1. Constraints on various $\Omega_b^X h^2$ from the Planck temperature and polarization data (68% and 95% confidence limits). We omit $\Omega_b^{\text{BBN}} h^2$ and $\Omega_b^{\text{HALO}} h^2$ that are not constrained by the data. The red/black stars represent mean $\Omega_b h^2$ values from the deuterium measurements (2)/(3).

further break (17) with terms that vanish when all Ω_b^X are identical, which makes using (17) impractical. For this reason we evaluate $\dot{\sigma}, \dot{\sigma}$ directly from the definition (16), iteratively substituting equations of motion for $\dot{h}, \dot{\eta}$ and other variables.

After finishing all the changes, we ensured that when we force all $\Omega_b^X h^2$ from Table I to be equal, we reproduce the standard CMB power spectra to better than 0.01%.

Note that agreement at a machine precision level is not expected, due to the c_s^2 breaking of (17) mentioned above.

IV. RESULTS

In this section we present our results, first when allowing all eight $\Omega_b^X h^2$ parameters to vary independently and

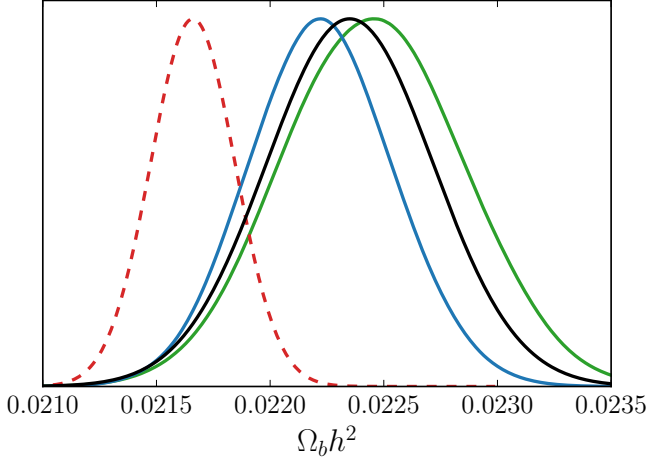


FIG. 2. Constraints on $\Omega_b^{\text{THO}} h^2$ (green) and $\Omega_b^R h^2$ (blue) from the Planck CMB power spectra when considering all eight $\Omega_b^X h^2$ independently. For comparison, values (2) and (3) derived from the deuterium abundance measurements are shown with red dashed and black lines, assuming Gaussian posteriors and with errors added in quadrature.

then when we are more restrictive and allow only three baryonic degrees of freedom.

A. Eight baryonic parameters

Running the CosmoMC with the Planck data when allowing all eight $\Omega_b^X h^2$ to vary, we find that $\Omega_b^{\text{BBN}} h^2$ and $\Omega_b^{\text{HALO}} h^2$ are not constrained by the data even within the very weak prior. This is in agreement with our expectations. In Figure 1 we show posterior probability distributions for the remaining six $\Omega_b^X h^2$. Of these, only $\Omega_b^{\text{THO}} h^2$ and $\Omega_b^R h^2$ are strongly constrained; the remaining ones are not competitive, with error bars at least four times larger. While we find that all $\Omega_b^X h^2$ constraints are in good agreement mutually and with the BBN constraint (3), weak tension is visible when compared with (2).

In Figure 2, we show the one-dimensional posterior probability distributions for the two well constrained parameters,

$$\Omega_b^{\text{THO}} h^2 = 0.02245 \pm 0.00040 \quad (18)$$

$$\Omega_b^R h^2 = 0.02222 \pm 0.00032, \quad (19)$$

together with the two BBN constraints. We see that the two constraints from Planck data are mutually consistent, which means that Planck data successfully passed our intended consistency test.

As another sanity check, we verified that the remaining cosmological parameters $A_s, \tau_{\text{rei}}, n_s, \Omega_c h^2, \theta_{\text{MC}}$ are consistent with their standard values, although with increased error bars. Looking particularly at constraints of H_0 , we see its value rise somewhat to

$$H_0 = (69.1 \pm 1.6) \text{ km/s/Mpc}. \quad (20)$$

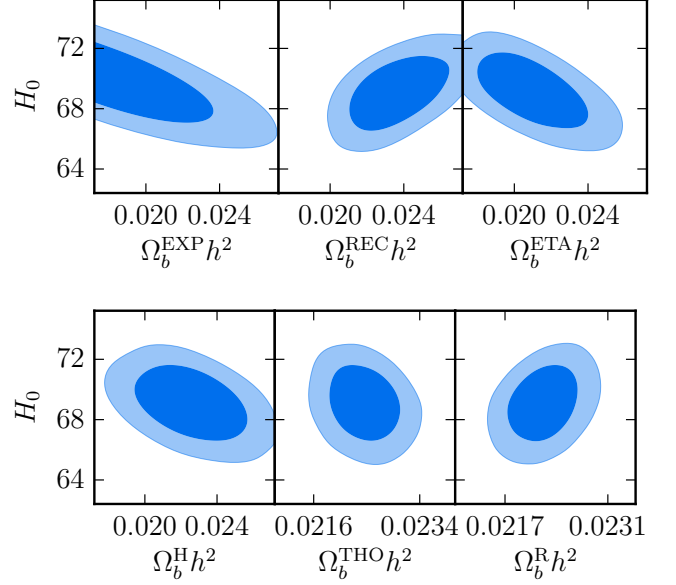


FIG. 3. Correlations between H_0 in km/s/Mpc and the six $\Omega_b^X h^2$ parameters constrained by Planck temperature and polarization data.

This is driven by Planck data preferring low $\Omega_b^{\text{EXP}} h^2$ and $\Omega_b^{\text{ETA}} h^2$ and high $\Omega_b^{\text{REC}} h^2$, see Fig. 3 for correlations between H_0 and the six $\Omega_b^X h^2$ parameters constrained by Planck.

B. Three baryonic parameters

Given we have pinned down the two physical processes that are responsible for constraining the density of baryons from the CMB, we can form a stronger consistency test by forcing all the remaining $\Omega_b^X h^2$ to be equal,

$$\Omega_b^{\text{EXP}} = \Omega_b^{\text{BBN}} = \Omega_b^{\text{REC}} = \Omega_b^{\text{ETA}} = \Omega_b^{\text{H}} = \Omega_b^{\text{HALO}}. \quad (21)$$

Running the CosmoMC with three baryonic densities allows us to constrain $\Omega_b^{\text{THO}} h^2$ and $\Omega_b^R h^2$ better as

$$\Omega_b^{\text{THO}} h^2 = 0.02241 \pm 0.00037 \quad (22)$$

$$\Omega_b^R h^2 = 0.02236 \pm 0.00021; \quad (23)$$

these results are also shown graphically in Fig. 4. Again, we find that the two ways in which Planck can constrain $\Omega_b h^2$ competitively are mutually consistent and also consistent with (3). The constraints actually appear to be *too* consistent, however this is unlikely to be anything but a coincidence.

Regarding the constraint on the Hubble constant, it drops back to

$$H_0 = (67.8 \pm 0.8) \text{ km/s/Mpc}, \quad (24)$$

close to its value in the standard analysis.

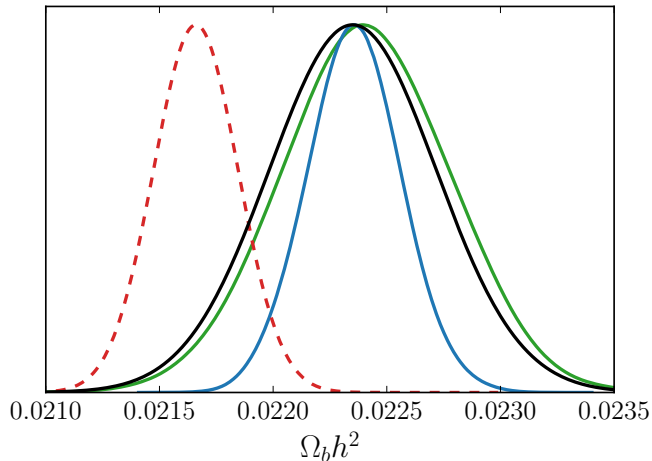


FIG. 4. Same as Fig. 2 when the six poorly constrained $\Omega_b^X h^2$ are forced to be identical (see (21)).

V. DISCUSSION

We went through the calculation of the CMB temperature and polarization power spectra and found eight distinct ways in which $\Omega_b h^2$ influences the result. By performing a Markov chain Monte Carlo analysis with the Planck temperature and polarization data, we found that $\Omega_b h^2$ is mostly constrained through the amplitude of Thomson scattering and through R , a coefficient en-

suring that Thomson scattering conserves momentum of the baryon-photon fluid.

Given both of these constraints are mutually consistent and also consistent with the empirical BBN constraint (3), we conclude that the proposed consistency test passed and Planck data are internally consistent from the point of view of $\Omega_b h^2$. This strengthens the robustness of the Planck $\Omega_b h^2$ constraints and thus further disfavors the BBN constraint (2).

In our analysis we uncovered that Thomson scattering amplitude $an_e \sigma_T$ is constrained at a 2% level. Instead of using this as a constraint on $\Omega_b h^2$, we can equivalently phrase it as σ_T changing its value by less than $\sim 2\%$ since the time of recombination. This is comparable to results of [16], who constrain this change to less than 0.5% by instead considering changes in the fine structure constant and all natural constants dependent on it, as opposed to just σ_T as we do.

We also found that the parameter R does not differ by more than $\sim 2\%$ from its standard model value, offering a $\sim 2\%$ test of momentum conservation in Thomson scattering during the epoch of recombination.

When we allow the eight $\Omega_b^X h^2$ parameters to differ, we obtain a value of H_0 (69.1 ± 1.6) km/s/Mpc, i.e. slightly higher than in the standard analysis, but still far away from the local measurement [3]. Restricting to three baryonic degrees of freedom mostly negates this preference for increased H_0 . Overall, the consistency of the various $\Omega_b h^2$ constraints means our analysis did not reveal any problem with the standard cosmological model.

-
- [1] N. Aghanim *et al.* (Planck), (2018), [arXiv:1807.06209 \[astro-ph.CO\]](#).
 - [2] R. J. Cooke, M. Pettini, and C. C. Steidel, *Astrophys. J.* **855**, 102 (2018), [arXiv:1710.11129 \[astro-ph.CO\]](#).
 - [3] A. G. Riess, S. Casertano, W. Yuan, L. M. Macri, and D. Scolnic, *Astrophys. J.* **876**, 85 (2019), [arXiv:1903.07603 \[astro-ph.CO\]](#).
 - [4] L. Knox and M. Millea, *Phys. Rev. D* **101**, 043533 (2020), [arXiv:1908.03663 \[astro-ph.CO\]](#).
 - [5] N. Aghanim *et al.* (Planck), (2019), [arXiv:1907.12875 \[astro-ph.CO\]](#).
 - [6] A. Lewis and S. Bridle, *Phys. Rev. D* **66**, 103511 (2002), [arXiv:astro-ph/0205436 \[astro-ph\]](#).
 - [7] A. Lewis, A. Challinor, and A. Lasenby, *Astrophys. J.* **538**, 473 (2000), [arXiv:astro-ph/9911177 \[astro-ph\]](#).
 - [8] P. Motloch and W. Hu, *Phys. Rev. D* **101**, 083515 (2020), [arXiv:1912.06601 \[astro-ph.CO\]](#).
 - [9] S. Dodelson, *Modern Cosmology* (Academic Press, Amsterdam, 2003).
 - [10] U. Seljak and M. Zaldarriaga, *Astrophys. J.* **469**, 437 (1996), [arXiv:astro-ph/9603033 \[astro-ph\]](#).
 - [11] A. Challinor and A. Lewis, *Phys. Rev. D* **71**, 103010 (2005), [arXiv:astro-ph/0502425 \[astro-ph\]](#).
 - [12] S. Seager, D. D. Sasselov, and D. Scott, *Astrophys. J.* **523**, L1 (1999), [arXiv:astro-ph/9909275 \[astro-ph\]](#).
 - [13] A. Mead, C. Heymans, L. Lombriser, J. Peacock, O. Steele, and H. Winther, *Mon. Not. Roy. Astron. Soc.* **459**, 1468 (2016), [arXiv:1602.02154 \[astro-ph.CO\]](#).
 - [14] F.-Y. Cyr-Racine and K. Sigurdson, *Phys. Rev. D* **83**, 103521 (2011), [arXiv:1012.0569 \[astro-ph.CO\]](#).
 - [15] M. C. Pookkillath, A. De Felice, and S. Mukohyama, *Universe* **6**, 6 (2019), [arXiv:1906.06831 \[astro-ph.CO\]](#).
 - [16] L. Hart and J. Chluba, (2019), [10.1093/mnras/staa412, arXiv:1912.03986 \[astro-ph.CO\]](#).